Journal of the Serbian Chemical Society
JSCS@tmf.bg.ac.rs • www.shd.org.rs/JSCS
J. Serb. Chem. Soc. 90 (2) 215–231 (2025)
JSCS–5831
Original scientific paper
Published 16 February, 2025

Malachite green removal by *Eryngium caeruleum* ash

SHAGHAYEGH AZIZI and HASSAN ZAVVAR MOUSAVI*

Department of Analytical Chemistry, Faculty of Chemistry, University of Guilan, P. O. Box 41335-1914, Rasht, Iran

(Received 15 April, revised 28 August, accepted 27 September 2024)

Abstract: In this study, malachite green (MG) has been successfully removed from an aqueous solution with the use of *Eryngium caeruleum* ash as an adsorbent. The influence of effective factors on the dye removal process, like contact time, the initial concentration of dye, amount of adsorbent, temperature and pH, has been studied. The results revealed that the optimal malachite green adsorption occurred at pH 7, 120 min of contact time, 0.01 g of adsorbent and 100 mg L^{-1} of initial dye concentration. Furthermore, the adsorption results follow the Langmuir isotherm with a correlation coefficient $R^2 = 0.98$ (q_{max} = = 476.19 mg g^{-1}) and pseudo–second order kinetic ($R^2 = 0.97$). Endothermic and spontaneous adsorption were implied by the positive $\Delta H°$, $\Delta S°$ and negative $\Delta G°$. Therefore, in order to remove MG from aqueous solutions, *E. caeruleum* ash can be exploited as a low-cost and environmentally friendly adsorbent.

Keywords: adsorption; low-cost adsorbent; isotherm; kinetics; thermosdynamics.

INTRODUCTION

Dyes are applied in many manufacturing sectors, which include food processing, pharmaceuticals, textiles, plastic, rubber and paper.[1] Furthermore, dyes are organic compounds and have high solubility in water, especially those classified as reactive, direct, acidic and basic, which makes it a problem to remove them with conventional methods. The existence of dyes in textile wastewater, in addition to harming the environment and water bodies, prevents the light penetration into the water, which ultimately causes the photosynthetic rate to decline and the level of dissolved oxygen to drop, endangering the lives of the aquatic creatures.[2,3] The malachite green dye is extensively used for several purposes in agriculture, health, food, textiles and other industries.

* Corresponding author. E-mail: hzmousavi@guilan.ac.ir
https://doi.org/10.2298/JSC240415083A

Due to its carcinogenicity, this dye is dangerous and poisonous for blue species, such as fish and mammals. The concentrations of malachite green increase with time and exposure to temperature and it also can cause many diseases, including cancer, respiratory poisoning, Chromosome breaks, gene mutations, *etc*. Therefore, it is necessary to remove and separate this colour before discharging dye wastewater into the water.[4] Furthermore, various pollutants are included in dye wastewater, such as salts, adhesives, acids and additives, which are toxic, carcinogenic, teratogenic and xenobiotic.[5,6] These features are responsible for the creation of allergic conjunctivitis, skin irritation, eye burns and occupational asthma in the human body.[7,8] Dyes are a significant sort of harmful substances that are easily recognized by the human eye. However, it is important to prevent the discharge of dyes into water sources. Various treatment technologies are employed in order to reach this goal. The adsorption process is also considered an effective and economical method due to its simplicity and accessibility.[9,10] Currently, the search to find the most effective technique, among many for dye removal, is active. The adsorption methods are frequently employed to remove specific types of contaminants from water, particularly those that are difficult to biodegrade. The surface adsorption cheap and easily accessible adsorbents have attracted the attention of many researchers and now they are looking for economical and effective methods, using synthetic and natural materials as adsorbents.[11] In this study, we used *Eryngium caeruleum* ash for removing the malachite green dye (MG) from aqueous solutions through the surface adsorption method.

EXPERIMENTAL

Materials

Each of the chemical substances has been procured from Merck. HCl (36 %) and sodium hydroxide granules of 99.9 % purity were used (M) for pH adjustment, whereas sodium chloride was used to measure the ionic strength. Malachite green (MG) dye was dissolved in distilled water as well.

Preparation of the MG dye solution

The adsorbate for this study was MG, a common cationic dye. MG, known by the chemical formula $C_{23}H_{26}N_2Cl$, is one of the dye derivatives of aniline with a solid green appearance. MG dye has been weighed and dissolved in distilled water to achieve a concentration of 600 ppm. The pH had been modified to 2–12 through the addition of 0.1 M HCl and NaOH solutions.

Preparation of the adsorbent

Initially, the *Eryngium caeruleum* was collected from mountainous regions and washed utilizing distilled water to eliminate all contaminants. Subsequently, the plant had been dried and subjected to gentle heat for crushing. Then that was placed in the oven to turn into ash after 6 h at 350 °C. The acquired ash was slightly ground and finally made into a fine powder and can be utilized as an adsorbent.

Adsorption studies

In this case, the batch adsorption studies have been carried out for studying the removal of MG dye by utilizing *E. caeruleum* ash as the adsorbent. All the parameters were considered fixed, and only the parameter that should be optimized was changed. 25 mL of MG dye solution was prepared and the effects of parameters such as adsorbent dosage (0.01–0.07 g), solution pH (2–12), initial dye concentration (100–500 mg L^{-1}), contact time (15–135 min) and the temperature (0–40 °C) were studied. The pH solutions were modified with the addition of 0.1 M HCl and NaOH solutions. The following formula has been used to compute the percentage removal and MG dye solution adsorption capacity:[12]

$$q_e = (C_0 - C_e)\frac{V}{W} \quad (1)$$

$$\text{Removal percentage} = 100\frac{C_0 - C_e}{C_0} \quad (2)$$

in which C_0 and C_e (mg L^{-1}) are the liquid-phase of the dye concentrations at the initiation and equilibrium, accordingly. W / g is the mass of dry sorbent used and V / L is solution volume.

Adsorption isotherms

To investigate and enhance the adsorption system design and understand the adsorption equilibrium, it is essential to study the adsorption isotherm. The adsorption isotherm at equilibrium describes the distribution of adsorbed molecules in solid and liquid phases. The adsorption isothermal models can be used for evaluating adsorption phenomena and predicting maximum adsorption capacity. Also, Freundlich, Langmuir and Temkin are the most applied:

$$R_L = \frac{1}{1 + k_L C_e} \quad (3)$$

Adsorption kinetics and mechanisms

For the determination of adsorption system and kinetics, different kinetic and adsorption models like pseudo-first and second-order models, internal particle diffusion, and Elovich kinetic models have been studied. Also, different correlation coefficient (R^2) values were calculated for various kinetic and isothermal models.

RESULTS AND DISCUSSION

SEM adsorbent characterization

Scanning electron microscope (SEM) images were used for the information on the morphology of the adsorbent. According to the images (Fig. 1), the *Eryngium caeruleum* ash has porous surfaces and a porous structure which makes them the suitable sites for the MG dye adsorption.

FT-IR adsorbent study

The FT-IR analysis was interpreted in order to investigate the functional groups included in the adsorbent. Fig. 2 reveals the FT-IR spectrum for the *E. caeruleum* ash. According to this analysis, the adsorption peaks within the spectral range of 1464 to 2962 cm^{-1} correspond to various functional groups, namely,

–CH_2– bending, N–H stretching amine, C–O carboxylic acid stretching, Si–O–Si stretching, O–H carboxylic acid, C–O–O peroxide stretching, C–S stretching, S–S stretching and C–H methyl stretching groups.[14–16]

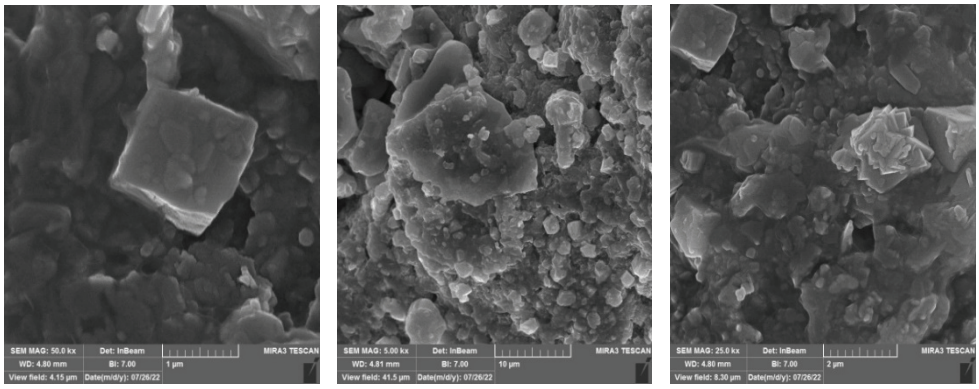

(a) (b) (c)

Fig. 1. *Eryngium caeruleum* ash adsorbent SEM images: a) 1, b) 10 and c) 2 µm mgnification.

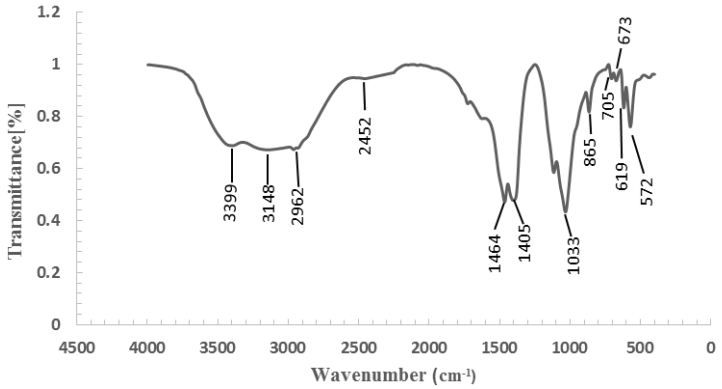

Fig. 2. The FT-IR spectrum for the *Eryngium caeruleum* ash.

Effect of solution pH

Several studies have shown that the initial solution pH can influence surface charge, the solubility of the adsorbate and the ionization degree in the adsorption method, so the initial solution pH is one of the main environmental factors. Diluted solutions of 0.1 M HCl and NaOH were added to 25 mL of MG dye solutions, which had a concentration of 100 mg L^{-1}, to optimize pH from 2–12. Then, 0.01 g of the adsorbent has been added to the flasks and agitated for 60 min on a shaker (at a constant 160 rpm shaking rate) at ambient temperature. The concentrations of the dye at equilibrium had been measured by a UV/Vis spectrophotometer (Perkin-Elmer, Junior model 35, U.S.) at 618 nm. The maximum MG dye

removal percentage (66.90 %) had been achieved at a pH of 7.0. Also, the zero point charge (pHzpc) value for *E. caeruleum* ash was found to be 6.0 (Fig. 3b). This result confirms that at a pH > pHzpc, the negative charge density on the MG dye surface increases, leading to MG elimination.[17] In fact, the adsorption capacity of MG dye is minimal in acidic solutions. This phenomenon could be attributed to the positive charge of the adsorbents, which leads to the repulsion of the cationic dye MG as they share the same charge.[18] According to Fig. 3a, at pH above 7, because of the existence of hydrogen bonds, the repulsive force between H^+ and cationic dye molecules causes a decrease in adsorption at first and then reaches a constant value.[19]

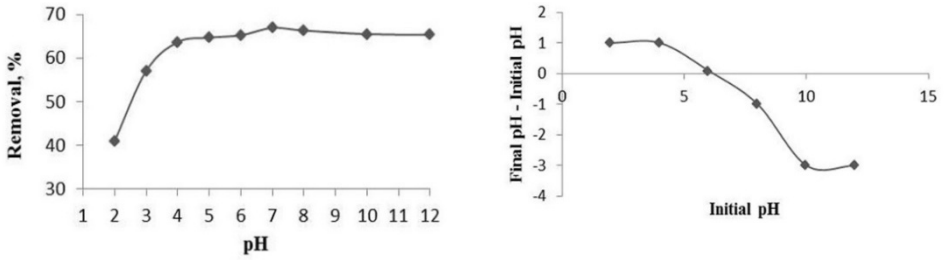

(a) (b)

Fig. 3. a) Effect of initial pH on MG adsorption; b) point of zero charge.

Effect of adsorbent dosage

The influence of changing the adsorbent dosage (0.005–0.07 g) on MG removal % is shown in Fig. 4. One key factor that significantly impacts the adsorption process and requires the examination in adsorption studies is the influence of the dosage of the adsorbent. In order to investigate this factor, MG dye solutions at 100 mg L^{-1} concentration were prepared in a volume of 25 mL under optimum pH 7 and then different doses of adsorbent in the range of 0.005 to 0.07 g were added to the dye solutions and they were stirred for 120 min at ambient temperature on a shaker (at a constant 160 rpm shaking rate). According to Fig. 4, the highest percentage of MG dye removal can be seen in the dosage of 0.01 g of adsorbent (74.12 %) since, in the graph after this point, the slope of the curve has reached an almost constant value. Therefore, the optimum dosage of adsorb-

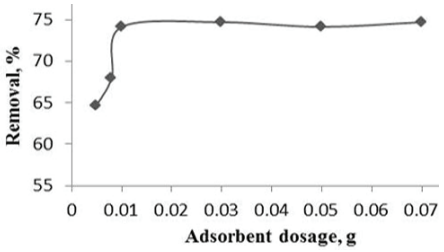

Fig. 4. Effect of adsorbent dosage on MG adsorption.

ent was considered to be 0.01 g because a higher adsorbent dosage can increase surface area.[20]

Effect of contact time

The optimal contact time should give enough time for the dye to adsorb the sites of the adsorbent surface so that the adsorption sites can adsorb the cationic dye molecules. To investigate this effect, 25 mL solutions of MG dye were prepared at a 100 mg L^{-1} concentration (pH 7). Also, 0.01 g of adsorbent has been added to the flasks and they have been stirred in the contact time range of 15 to 135 min at ambient temperature on a shaker (at a constant 160 rpm shaking rate). Fig. 5 displays the influence of contact time on the MG adsorption. Initially, the curve slope is steeper, considering the accessibility of the unoccupied adsorbent sites. However, the line's slope smooths after 120 min and the MG dye removal percentage remains constant. In other words, as time increases, the percentage of MG removal increases and after a while, it starts to rise with less intensity and then it reaches a constant value. After 120 min, the unoccupied sites on the adsorbent surface are saturated with the pollutant and the adsorption system reaches equilibrium. As a result, the optimal contact time was 120 min with 74.12 % MG dye removal.

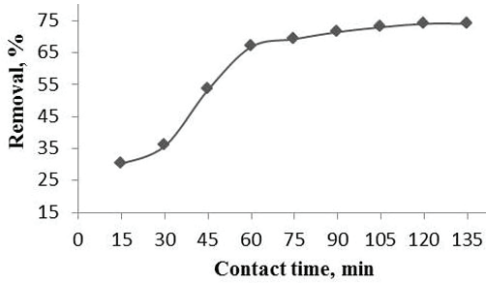

Fig. 5. Effect of contact time on MG adsorption.

Effect of initial concentration

Fig. 6 shows that variations in the initial dye concentration can influence the percentage removal of the MG. To investigate this effect, 25 mL solutions of MG dye were prepared at various concentrations (100–500 mg L^{-1} at pH 7). Then, 0.01 g of adsorbent has been added to the solutions and they have been stirred for 120 min at ambient temperature on a shaker (at a constant 160 rpm shaking rate). According to Fig. 6, at low concentrations, fewer pollutants were present in the solution and more sites on the adsorbent surface were ready to accept dye molecules. However, after the increase in dye concentration, a large number of adsorbed molecules competed to occupy the empty sites on the adsorbent and consequently, the percentage of dye removal decreased.[21] Therefore, the concen-

tration of 100 ppm (74.17 removal %) was considered as the optimal concentration.

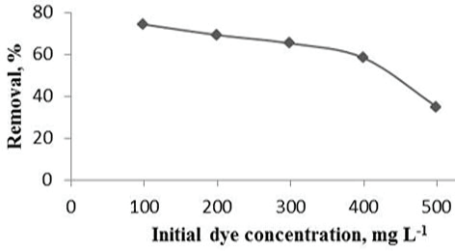

Fig. 6. Effect of initial dye concentration on MG adsorption.

Effect of temperature

The temperature is an essential parameter in determining the adsorbent capacity for physical and chemical adsorption.[22] In fact, temperature can provide useful information about thermodynamic parameters. In order to test the temperature factor, 100 mg L^{-1} of the MG solutions were prepared under conditions of pH 7 in a volume of 25 mL. Also, 0.01 g of adsorbent was added to flasks and the solutions were stirred for 120 min. According to Fig. 7, the studied temperature range was 0 up to 40 °C. The results show that as the temperature increases, the viscosity of the MG dye solution decreases, which can lead to a higher diffusion rate of MG dye molecules in the outer boundary layers and facilitate their penetration into the inner pores of the absorbent. Therefore, the optimal adsorption temperature is 40 °C. (313 K, removal 99.87 %).

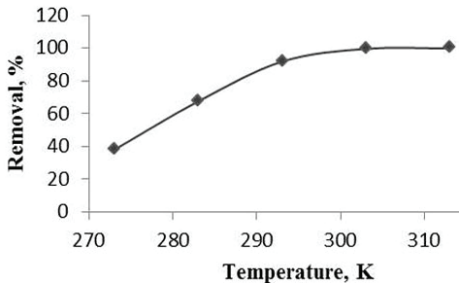

Fig. 7. Effect of temperature on MG adsorption.

Effect of ionic strength

In addition to dyes, textile wastewater contains various types of ions and these ions can be effective in removing dyes through surface adsorption. In order to study this parameter, 25 mL of MG dye solutions at pH 7 (concentration of 100 mg L^{-1}) were prepared, then 0.01 g of adsorbent was added to solutions. Then 2 mL of NaCl with concentrations of 0.1, 0.3, 0.6 and 1 M was added to each of these prepared solutions and they were agitated for 120 min at ambient temperature on a shaker (at a constant 160 rpm shaking rate). According to Fig.

8, as the sodium chloride concentration increases, the percentage of MG dye removed decreases and this is due to the competition between sodium ions and contaminant molecules to occupy all accessible sites.[23]

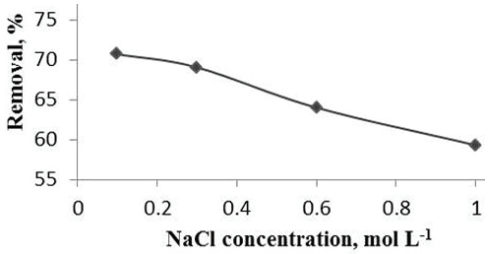

Fig. 8. Effect of ionic strength on MG dye adsorption.

Adsorption isotherms studies

The efficiency of adsorbents used for the adsorption can be investigated using adsorption isotherms such as Freundlich, Langmuir and Temkin and it is also possible to determine the nature of the interaction between the adsorbent and the adsorbate material.[24]

Langmuir adsorption isotherm

The maximum adsorbent capacity was calculated using the Langmuir isotherm model and is shown as follows: [25]

$$\frac{C_e}{q_e} = \frac{1}{K_L q_{max}} + \frac{C_{eq}}{q_{max}} \tag{4}$$

where q_e is the amount of adsorbate at equilibrium, q_{max} / mg g^{-1} is the maximum capacity of adsorbent, K_L / L mg^{-1} is the Langmuir isotherm constant that refers to the adsorption rate and C_e / mg L^{-1} is the equilibrium adsorbate concentration. Through the charting of C_e/q_e *versus* C_e, q_{max} and K_L values were obtained. The fundamental characteristics of a Langmuir isotherm could be defined through a dimensionless parameter recognized as the separation factor R_L, which value was found to be 0.14. The $R_L < 1$ means that the adsorption of MG is favourable in this investigated study. The Langmuir adsorption isotherm diagram can also be seen in Fig. 9. Table I shows that the adsorption process follows the Langmuir isotherm ($R^2 = 0.98$) with a q_{max} of 476.19 mg g^{-1}.

Freundlich adsorption isotherm

In the Freundlich isotherm model, adsorption can occur on the heterogeneous surface of the adsorbent with a non-uniform distribution of heat. The following formula refers to the linear form of this model:[26]

$$\ln q_e = \ln K_F + \frac{1}{n} \ln C_e \tag{5}$$

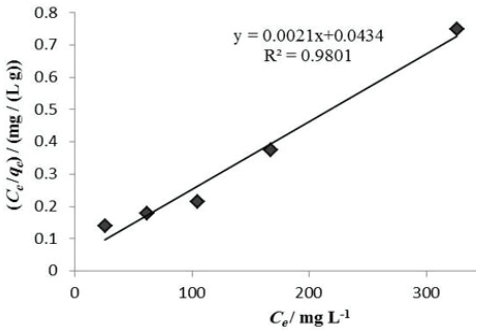

Fig. 9. Langmuir *Eryngium caeruleum* ash plot for adsorption of MG.

TABLE I. Equilibrium isotherm modeling of MG adsorption onto *Eryngium caeruleum* ash

Isotherm	*Eryngium caeruleum* ash
Langmuir	
q_{max} / mg g^{-1}	476.19
K_L	0.04
R_L	0.14
R^2	0.98
Freundlich	
N	2.64
K_F / L mg^{-1}	67.26
R^2	0.67
Temkin	
B / J mol^{-1}	122.39
K_T / L mg^{-1}	0.28
R^2	0.61

where q_e is the adsorbed amount of dye at equilibrium, K_F and $1/n$ are the Frendulich constants and C_e is the equilibrium concentration. The values of $1/n$ express the non-linearity of the relationship between the solution concentration and the adsorption. When the value of n is less than one and n is greater than one, chemical adsorption and physical adsorption are implied, respectively. And also, if $n = 1$, adsorption is linear. Fig. 10 shows ln q_e *versus* ln C_e plotted for MG adsorption on the adsorbent. The values of n and K_F are computed using the

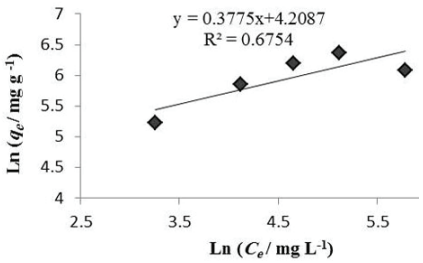

Fig. 10. Freundlich *Eryngium caeruleum* ash plot for adsorption of MG.

slope and the intercept separately, which were (2.64) and (67.26 mg g^{-1}) and also R^2 = 0.67 was obtained, which did not seem appropriate. As a result, since the value of n >1 the adsorption has been carried out as a chemical process.

Temkin adsorption isotherm

Variations in adsorption energy and the adsorbent surface were evaluated utilizing the Temkin adsorption isotherm. The R^2 value has been used as a criterion for effectiveness and efficiency. The Temkin isothermal model is shown using the following linear formula:[27]

$$q_e = \frac{RT}{b} \ln K_T + \frac{RT}{b} \ln C_e \quad (6)$$

where R, 8.314 J mol^{-1} K^{-1}, is the universal constant of the gas and T / K represents temperature (absolute).[24] The Temkin isotherm model of MG dye adsorption onto *E. caeruleum* ash is shown in Fig. 11 by charting q_e *versus* ln C_e at a constant temperature. According to Table I, R^2 for the Temkin isotherm model is 0.61. The results show that the Langmuir isotherm is more accurate than other isotherms in describing the adsorption of MG dye on the adsorbent.

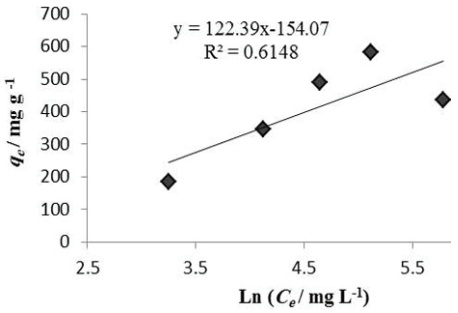

Fig. 11. Temkin *Eryngium caeruleum* ash plot for adsorption of MG.

Adsorption kinetic study

To provide information about the factors that impact reaction speed, it is necessary to carry out kinetic evaluations. In this study, various kinetic models have been used for the analysis of the data to investigate the mechanisms of MG dye adsorption on the adsorbent, including Elovich, intra-particle, pseudo-first order and pseudo-second order.

Pseudo-first-order kinetic model

In surface adsorption studies, the pseudo-first-order is an old kinetic model and can give information about the adsorption kinetics of pollutants.[28] Pseudo-first-order rate equations were typically used to describe the adsorbate performance from the tested dye solution. The linear model of this kinetic model is provided using the following equation: [29]

$$\ln(q_e - q_t) = \ln q_e - k_1 t \quad (7)$$

where q_e / mg g^{-1} is the amount of dye adsorbate on the adsorbent surface at equilibrium, q_t / mg g^{-1} is the amount of dye adsorbed at time t / min and k_1 / min^{-1} is the rate constant. Fig. 12 shows the pseudo-first-order model of the adsorption of MG dye onto *E. caeruleum* ash by charting ln $(q_e - q_t)$ *versus* contact time. According to Table II, k_1 and q_e were calculated and R^2 for this kinetic model was 0.90.

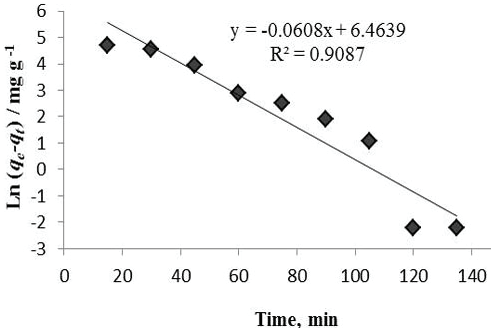

Fig. 12. Pseudo-first-order model of MG adsorption onto *Eryngium caeruleum* ash.

TABLE II. Adsorption kinetic models of MG adsorption onto *Eryngium caeruleum* ash

Adsorption kinetic model	Constant	MG dye
Pseudo-first-order	q_e / mg g^{-1}	641.55
	k_1 / min^{-1}	0.06
	R^2	0.90
Pseudo-second-order	q_e / mg g^{-1}	243.90
	k_1 / min^{-1}	0.004
	R^2	0.97
Elovich kinetic	α / g mg^{-1}	14.09
	β / mg g^{-1} min^{-1}	0.017
	R^2	0.92
Intraparticle-diffusion	K_{id} / mg g^{-1}min$^{-1/2}$	15.47
	C / mg g^{-1}	23.8
	R^2	0.88

Pseudo-second-order kinetic model

The pseudo-second-order model is another model applied for analysing the adsorption kinetics. The linear equation for the model is as follows:[30]

$$\frac{t}{q_t} = \frac{1}{k_2 q_e^2} + \frac{t}{q_e} \quad (8)$$

where k_2 / g mg $^{-1}$ min^{-1} is the constant rate and t / min is the contact time. Fig. 13 shows the charting of t/q_t *versus* contact time and according to Table II, R^2 for this kinetic model obtained 0.97. The data indicate that the second-order kinetic

equation can provide a suitable description of the MG adsorption mechanism on the surface of the adsorbent.

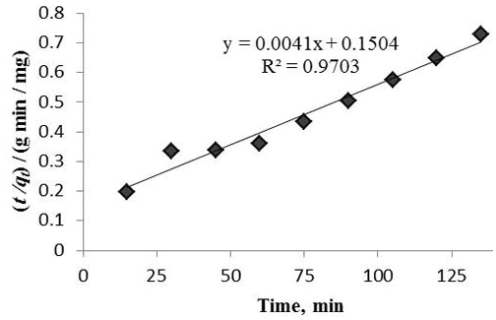

Fig. 13. Pseudo-second-order model of MG adsorption onto *Eryngium caeruleum* ash.

Elovich kinetic model

Elovich is a kinetic equation that has been used to evaluate boron adsorption. This model has the following linear formula:[31]

$$q_t = \frac{1}{\beta}\ln(\alpha\beta) + \frac{1}{\beta}\ln t \tag{9}$$

where α is the chemisorption rate at zero coverage and β is associated with both chemical adsorption activation energy and the extent of surface coverage. Fig. 14 shows the Elovich model of MG dye adsorption onto *E. caeruleum* ash by charting q_t *versus* ln t. According to Table II, R^2 for the Elovich kinetic model is 0.92, which shows that this kinetic model has a suitable correlation coefficient.

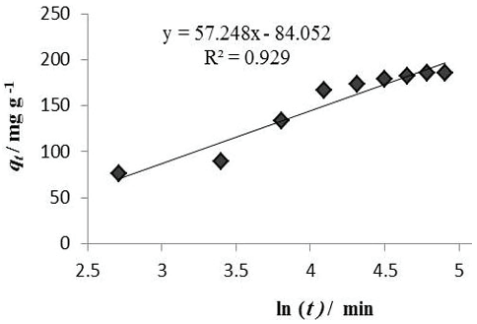

Fig. 14. Elovich kinetic model of MG adsorption onto *Eryngium caeruleum* ash.

Intraparticle-diffusion kinetic model

Fig. 15 shows the intraparticle diffusion model of MG dye adsorption onto *E. caeruleum* ash by charting q_t *versus* $t^{0.5}$. This is a kinetic model based on diffusion, which has the following equation:[32]

$$q_t = k_{\mathrm{id}} t^{0.5} + C \tag{10}$$

where K_{id} / mg g^{-1} min$^{-1/2}$ the constant rate, q_t / mg g^{-1} is the fraction adsorbate uptake at time and C / mg g^{-1} is the intercept that gives information about the thickness of the boundary layers surrounding the adsorbent. According to Table II, R^2 for this kinetic model is 0.88.

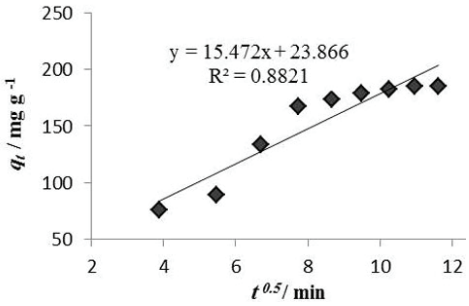

Fig. 15. Intraparticle diffusion model of MG adsorption onto *Eryngium caeruleum* ash.

Thermodynamic study

In this study, the thermodynamic equations were used to investigate the effect of temperature on the adsorption of MG on the adsorbent surface. In fact, to increase the efficiency of the adsorption process, thermodynamic studies were performed. Thermodynamic parameters can be obtained using the following formulas:[33]

$$\Delta G^{\circ} = -RT \ln K_d \tag{11}$$

$$\ln K_d = \frac{\Delta S^{\circ}}{R} - \frac{\Delta H^{\circ}}{RT} \tag{12}$$

where T / K is is the absolute solution temperature and K_d is the equilibrium constant. The spontaneity or non-spontaneity of the adsorption system is inferred from the change in Gibbs energy. According to Table III, by increasing the temperature in the range of 273–303 K, it was found that the values of $\Delta G°$ decreased from –0.978 to –0.198 kJ mol^{-1}. Therefore, at higher temperatures, the adsorption of the MG dye is spontaneous and more favourable.[23] According to the intercept and slope of the plot in Fig. 16, the parameters of the thermodynamic process, namely $\Delta H°$ and $\Delta S°$ were calculated and the positive value for $\Delta H°$ indicates an endothermic adsorption process. Considering that $\Delta S° > 0$, the

TABLE III. Thermodynamic study of MG adsorption onto *Eryngium caeruleum* ash

T / K	K_d	$\Delta G°$ / kJ mol^{-1}	$\Delta H°$ / kJ mol^{-1}	$\Delta S°$ / J mol^{-1} K^{-1}	R^2
273	1.538718291	–0.978136222	136.02	497.817	0.9661
283	5.207006369	–3.882234294			
293	28.2106599	–8.135515677			
303	669.7222222	–16.39171195			
313	2014.166667	–19.79805951			

affinity of the adsorbent for MG dye decreased and it was found that the randomness of the solid / solution interface increased during adsorption.

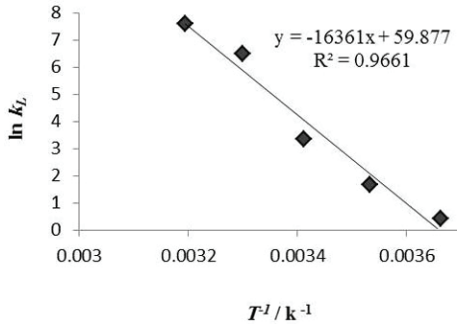

Fig. 16. Thermodynamic study of MG dye adsorption onto *Eryngium caeruleum* ash.

Comparison of the various adsorbents to remove MG dye

Table IV shows various adsorbents used for MG dye removal and it was concluded that the *E. caeruleum* ash adsorbent has been able to allocate the maximum adsorption capacity, compared to other adsorbents, which indicates that this adsorbent is suitable to remove MG dye from an aqueous solution.

TABLE IV. Comparison of the various adsorbents to remove MG dye

Adsorbent	Adsorption capacity mg g^{-1}	pH	Ref.
Almond gum	172.41	7	34
Sulfuric acid-treated coffee husk (ACH)	264.82	6.8	35
Activated carbon from apricot stone (ASM)	88.5	10	36
Elaeagnus Stone Activated Carbon (EAC)	432.90	7	37
Nanochitosan from shrimp shells (STP)	317.73	6	38
Carbonised pomegranate peel (CPP)	31.45	6	24
Carica papaya wood	52.63	10	39
Activated carbon from pistachio shell (PisAC)	76.92	7	40
Eryngium caeruleum ash	476.19	7	This study

CONCLUSIONS

Recently, researchers have been interested in finding cost-effective adsorbents for wastewater treatment. The structural and morphological characteristics of *Eryngium caeruleum* ash were investigated using FT-IR and SEM. Various experimental parameters like initial concentration of the dye, equilibrium contact time, temperature, dosage of the adsorbent and pH of dye solution, were investigated. The optimum efficiency for MG removal using *E. caeruleum* ash was observed at pH 7, dosage of 0.01 g, contact time of 120 min, initial MG concentration of 100 ppm and temperature of 40 °C. The adsorption process of MG dye onto the adsorbent was fitted with the pseudo-second-order kinetics model and

the Langmuir isotherm model and the q_{max} has been attained at 476.19 mg g^{-1}. The adsorption procedure, supported due to the negative $\Delta G°$ and positive $\Delta H°$ values, was identified as spontaneous, chemisorptive and endothermic. According to this study, *E. caeruleum* ash, in addition to being low-cost, easy to access, easy to prepare and preventing the spread of pollution in the environment, is also environmentally friendly. Therefore, this adsorbent can remove malachite green dye from aqueous solutions.

Acknowledgment. Thanks to the Chemistry Department of Guilan University for providing laboratory facilities.

И З В О Д

УКЛАЊАЊЕ МАЛАХИТ-ЗЕЛЕНЕ БОЈЕ ПЕПЕЛОМ *Eryngium caeruleum*

SHAGHAYEGH AZIZI и HASSAN ZAVVAR MOUSAVI

Department of Analytical Chemistry, Faculty of Chemistry, University of Guilan, P. O. Box 41335-1914, Rasht, Iran

Малахит зелена боја је успешно уклоњена из воденог раствора употребом пепела *Eryngium caeruleum* као адсорбента. Испитиван је утицај ефективних фактора на процес уклањања боје, као што су време контакта, почетна концентрација боје, количина адсорбенса, температура и pH. Добијени резултати показују да су оптимални услови за адсорпцију малахит зелене боје: pH 7, време контакта 120 min, количина адсорбенса 0,01 g, почетна концентрација боје 100 mg mL^{-1}. Такође, резултати су у складу са Лангмуировом изотермом (R^2 = 0,98), (q_{max} = 476,19 mg g^{-1}), и кинетиком псеудо-другог реда (R^2 = 0,97). Ендотермна и спонтана адсорпција су имплициране позитивним $\Delta H°$ и $\Delta S°$ вредностима, као и негативним $\Delta G°$. Добијени резултати указују да за уклањање малахит зелене боје из водених раствора може да се примени јефтин и еколошки прихватљив адсорбенс пепео *E. caeruleum*.

(Примљено 15. априла, ревидирано 28. августа, прихваћено 27. септембра 2024)

REFERENCES

1. M. Zarrabi, R. Alizadeh, S. Mahboob, *Sep. Purif. Technol*. **211** (2019) 738 (https://doi.org/10.1016/j.seppur.2018.10.026)
2. M. M. Hassan, C. M. Carr, *Chemosphere* **209** (2018) 201 (https://doi.org/10.1016/j.chemosphere.2018.06.043)
3. M. Imran, D.E. Crowley, A. Khalid, S. Hussain, M.W. Mumtaz, M. Arshad, *Rev. Environ. Sci. Biotechnol*. **14** (2015) 73 (https://doi.org/10.1007/s11157-014-9344-4)
4. K. Tewari, G. Singhal, R. K. Arya, *Rev. Chem. Eng*. **34** (2018) 427 (https://doi.org/10.1515/revce-2016-0041)
5. K. Jain, A. S. Patel, V. P. Pardhi, S. J. S. Flora, *Molecules* **26** (2021) 1797 (https://doi.org/10.3390/molecules26061797)
6. D. A. Yaseen, M. Scholz, *Int. J. Environ. Sci. Technol*. **16** (2019) 1193 (https://doi.org/10.1007/s13762-018-2130-z)
7. D. Ma, H. Yi, C. Lai, X. Liu, X. Huo, Z. An, L. Li, Y. Fu, B. Li, M. Zhang, L. Qin, S. Liu, L. Yang, *Chemosphere* **275** (2021) 130104 (https://doi.org/10.1016/j.chemosphere.2021.130104)

8. F. E. Titchou, H. Zazou, H. Afanga, J. El Gaayda, R. Ait Akbour, P. V. Nidheesh, M. Hamdani, *Chem. Eng. Process. – Process Intensif.* **169** (2021) 108631 (https://doi.org/10.1016/j.cep.2021.108631)
9. A. Khaligh, H. Zavvar Mousavi, A. Rashidi, H. Shirkhanloo, *J. Serb. Chem. Soc.* **83** (2018) 651 (https://doi.org/10.2298/JSC170827112K)
10. A. A. Fodeke and O. O. Olayera, *J. Serb. Chem. Soc.* **84** (2019) 1143 (https://doi.org/10.2298/JSC190209042F)
11. W. Wei, L. Yang, W. H. Zhong, S. Y. Li, J. Cui, Z. G. Wei, *Dig. J. Nanomater. Biostruct.* **19** (2015) 1343 (https://www.chalcogen.ro/1343_Wei.pdf)
12. S. Farch, M. M. Yahoum, S. Toumi, H. Tahraoui, S. Lefnaoui, M. Kebir, M. Zamouche, A. Amrane, J. Zhang, A. Hadadi, L. Mouni, *Separations* **10** (2023) 60 (https://doi.org/10.3390/separations10010060)
13. A. B. D. Nandiyanto, W. C. Nugraha, I. Yustia, R. Ragadhita, M. Fiandini, M. Saleh, D. R. Ningwulan, *J. Adv. Res. Appl. Mech.* **106** (2023) 1 (https://doi.org/10.37934/aram.106.1.113)
14. A. B. D. Nandiyanto, R. Oktiani, R. Ragadhita, *Indones. J. Sci. Technol.* **4** (2019) 97 (https://doi.org/10.17509/ijost.v4i1.15806)
15. J. Coates, *Encycl. Anal. Chem.* **12** (2000) 10815 (https://doi.org/10.1002/9780470027318.a5606)
16. E. Smidt, M. Schwanninger, *Spectrosc. Lett.* **38** (2005) 247
17. (https://doi.org/10.1081/SL-200042310)
18. R. Bagheri, M. Ghaedi, A. Asfaram, E. A. Dil, H. Javadian, *Polyhedron* **171** (2019) 464 (https://doi.org/10.1016/j.poly.2019.07.037)
19. M. Messaoudi, M. Douma, N. Tijani, Y. Dehmani, L. Messaoudi, *Desalin. Water Treat.* **240** (2021) 191 (https://doi.org/10.5004/dwt.2021.27688)
20. U. Jinendra, B. M. Nagabhushana, D. Bilehal, *Desalin. Water Treat.* **209** (2021) 392 (https://doi.org/10.5004/dwt.2021.26536)
21. N. Khamis Soliman, A. F. Moustafa, A. A. Aboud, K. S. A. Halim, *J. Mater. Res. Technol.* **8** (2019) 1798 (https://doi.org/10.1016/j.jmrt.2018.12.010)
22. N. M. Mahmoodi, Z. Mokhtari Shourijeh, *Desalin. Water Treat.* **57** (2016) 20076 (https://doi.org/10.1080/19443994.2015.1109562)
23. Y. Miyah, A. Lahrichi, M. Idrissi, K. Anis, R. Kachkoul, N. Idrissi, S. Lairini, V. Nenov, F. Zerrouq, *J. Mater. Environ. Sci*. **8** (2017) 3570 (https://www.jmaterenvironsci.com/Document/vol8/vol8_N10/377-JMES-Myah.pdf)
24. D. R. Rout, H. M. Jena, *Mater. Today* **47** (2021) 1173 (https://doi.org/10.1016/j.matpr.2021.03.406)
25. F. Gündüz, B. Bayrak, *J. Mol. Liq.* **243** (2017) 790 (https://doi.org/10.1016/j.molliq.2017.08.095)
26. D. C. Roy, M. M. Sheam, M. R. Hasan, A. K. Saha, A. K. Roy, M. E. Haque, M. M. Rahman, T. Swee-Seong, S. K. Biswas, *bioRxiv* (2020) 2020 (https://doi.org/10.1101/2020.03.29.014274)
27. S. Archana, B. K. Jayanna, A. Ananda, M. S. Ananth, A. M. Ali, H. B. Muralidhara, K. Y. Kumar, *J. Indian Chem. Soc.* **99** (2022) 100249 (https://doi.org/10.1016/j.jics.2021.100249)
28. Y. Dehmani, O. El Khalki, H. Mezougane, S. Abouarnadasse, *Chem. Data Collect.* **33** (2021) 100674 (https://doi.org/10.1016/j.cdc.2021.100674)
29. D. R. Rout, H. M. Jena, *Environ. Sci. Pollut. Res.***30** (2023) 22992 (https://doi.org/10.1007/s11356-022-23774-3)

30. J. U. Ani, S. C. Agbo, O. A. Odewole, F. K. Ojo, O. L. Alum, K. G. Akpomie, A. C. Ofomatah, H. O. Chukwuemeka-Okorie, O. D. Onukwuli, *IOP Conf. Ser.: Earth Environ. Sci*. **1178** (2023) 012023 (https://doi.org/10.1088/1755-1315/1178/1/012023)
31. S. Ukachuku, E. D. Dikio, *World News Nat. Sci.* **49** (2023) 1 (http://www.worldnewsnaturalsciences.com/wp-content/uploads/2023/05/WNOFNS-49-2023-1-13.pdf)
32. E. H. Gürkan, B. İlyas, Y. Tibet, *Int. J. Environ. Anal. Chem*. **103** (2023) 1343 (https://doi.org/10.1080/03067319.2021.1873314)
33. S. S. Madan, K. L. Wasewar, C. Ravi Kumar, *Adv. Powder Technol*. **27** (2016) 2112 (https://doi.org/10.1016/j.apt.2016.07.024)
34. A. I. Abd-Elhamid, H. F. Aly, H. A. Soliman, A. A. El-Shanshory, *J. Mol. Liq*. **265** (2018) 226 (https://doi.org/10.1016/j.molliq.2018.05.127)
35. F. Bouaziz, M. Koubaa, F. Kallel, R. E. Ghorbel, S. E. Chaabouni, *Int. J. Biol. Macromol*. **105** (2017) 56 (https://doi.org/10.1016/j.ijbiomac.2017.06.106)
36. T. K. Murthy, B. S. Gowrishankar, M. C. Prabha, M. Kruthi, R. H. Krishna, *Microchem. J.***146** (2019) 192 (https://doi.org/10.1016/j.microc.2018.12.067)
37. M. Abbas, *Adsorpt. Sci. Technol*. **38** (2020) 24 (https://doi.org/10.1177/0263617420904476)
38. Ü. Geçgel, O. Üner, G. Gökara, Y. Bayrak, *Adsorpt. Sci. Technol*. **34** (2016) 512 (https://doi.org/10.1177/0263617416669727)
39. S. Salamat, M. Hadavifar, H. Rezaei, *J. Environ. Chem. Eng.* **7** (2019) 103328 (https://doi.org/10.1016/j.jece.2019.103328)
40. S. Rangabhashiyam, S. Lata, P. Balasubramanian, *Surf. Interfaces* **10** (2018) 197 (https://doi.org/10.1016/j.surfin.2017.09.011)
41. H. Mahadevan, P. V. M. Nimina, K. A. Krishnan, *Sustain. Water Resour. Manage*. **8** (2022) 38 (https://doi.org/10.1007/s40899-022-00612-5).